Large-Scale Domain Conformational Change Is Coupled to the Activation of the Co−C Bond in the B$_{12}$-Dependent Enzyme Ornithine 4,5-Aminomutase: A Computational Study
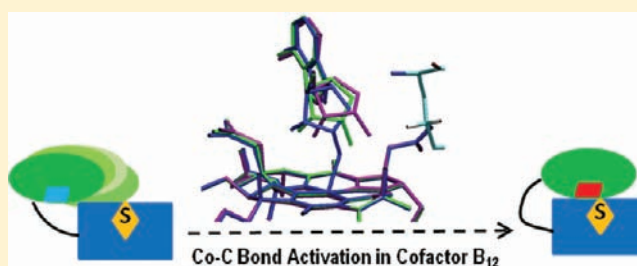
Jiayun Pang,*[†,‡,§] Xin Li,[⊥] Keiji Morokuma,[⊥] Nigel S. Scrutton,[‡,‖] and Michael J. Sutcliffe*[‡,§]

[‡]Manchester Interdisciplinary Biocentre, [§]School of Chemical Engineering and Analytical Science, and [‖]Faculty of Life Sciences, University of Manchester, 131 Princess Street, Manchester M1 7DN, United Kingdom
[⊥]Fukui Institute for Fundamental Chemistry, Kyoto University, Kyoto 606-8103, Japan

ⓈSupporting Information

ABSTRACT: We present here an energetic and atomistic description of how D-ornithine 4,5-aminomutase (OAM), an adenosylcobalamin (AdoCbl; coenzyme B$_{12}$)-dependent isomerase, employs a large-scale protein domain conformational change to orchestrate the homolytic rupture of the Co−C bond. Our results suggest that in going from the open form (catalytically inactive) to the closed form (catalytically active), the Rossmann domain of OAM effectively approaches the active site as a rigid body. It undergoes a combination of a ~52° rotation and a ~14 Å translation to bring AdoCbl—

Co-C Bond Activation in Cofactor B$_{12}$

initially positioned ~25 Å away—into the active-site cavity. This process is coupled to repositioning of the Ado moiety of AdoCbl from the eastern conformation to the northern conformation. Combined quantum mechanics and molecular mechanics calculations further indicate that in the open form, the protein environment does not impact significantly on the Co−C bond homolytic rupture, rendering it unusually stable, and thus catalytically inactive. Upon formation of the closed form, the Co−C bond is activated through the synergy of steric and electrostatic effects arising from tighter interactions with the surrounding enzyme. The more pronounced effect of the protein in the closed form gives rise to an elongated Co−C bond (by 0.03 Å), puckering of the ribose and increased "strain" energy on the Ado group and to a lesser extent the corrin ring. Our computational studies reveal novel strategies employed by AdoCbl-dependent enzymes in the control of radical catalysis.

1. INTRODUCTION

Enzyme catalysis is an intrinsically dynamic process, where a direct link between domain motions that occur on a time scale of micro- to milli-second and enzymatic function has been established. These large-scale domain motions are coupled to the catalytic cycle by facilitating substrate binding/product release and by modulating favorable active-site architecture that protects the transient chemically active intermediates.[1−4] Adenosylcobalamin (AdoCbl; coenzyme B$_{12}$) is nature's radical repository designed to catalyze challenging chemical reactions by generating reactive free radical intermediates.[5] The catalytic strategies employed by the family of AdoCbl-dependent enzymes to reinforce the control of highly reactive radical intermediates have long intrigued biochemists and chemists alike.[6−18] Using a variety of computational approaches, we present here an energetic and atomistic description of how D-ornithine 4,5-aminomutase (OAM), an AdoCbl-dependent isomerase, employs a large-scale protein domain conformational change to orchestrate the homolytic rupture of the Co−C bond.

OAM is a class-III AdoCbl-dependent isomerase. It participates in the oxidative fermentation of L-ornithine by converting D-ornithine to 2,4-diaminopentanoate.[19] In addition to

AdoCbl, OAM also employs cofactor pyridoxal L-phosphate (PLP) which forms an internal aldimine link with Lys629 in the resting state of the enzyme and then forms an external aldimine link with the incoming substrate (see Figure 1 for the proposed reaction scheme).[20,21] Previous computational studies suggest that the role of PLP is to lower the energy barrier for the conversion of radical intermediates by (1) introducing a double bond that connects to the migrating amine and (2) the electron withdrawing function of the pyridine ring.[14,22] In the proposed reaction scheme (Figure 1), homolysis of the Co−C bond triggered by substrate binding generates cob(II)alamin radical and the transient carbon-centered 5′-deoxyadenosyl radical (Ado-CH$_2$•), which subsequently abstracts hydrogen from the PLP-bound substrate. This produces a substrate radical that isomerizes to form a product-like radical. Reabstraction of the hydrogen from the 5′-deoxyadenosine (Ado-CH$_3$) by the product-like radical produces Ado-CH$_2$• which recombines with the cob(II)alamin radical to regenerate the AdoCbl Co−C bond, completing the catalytic cycle.
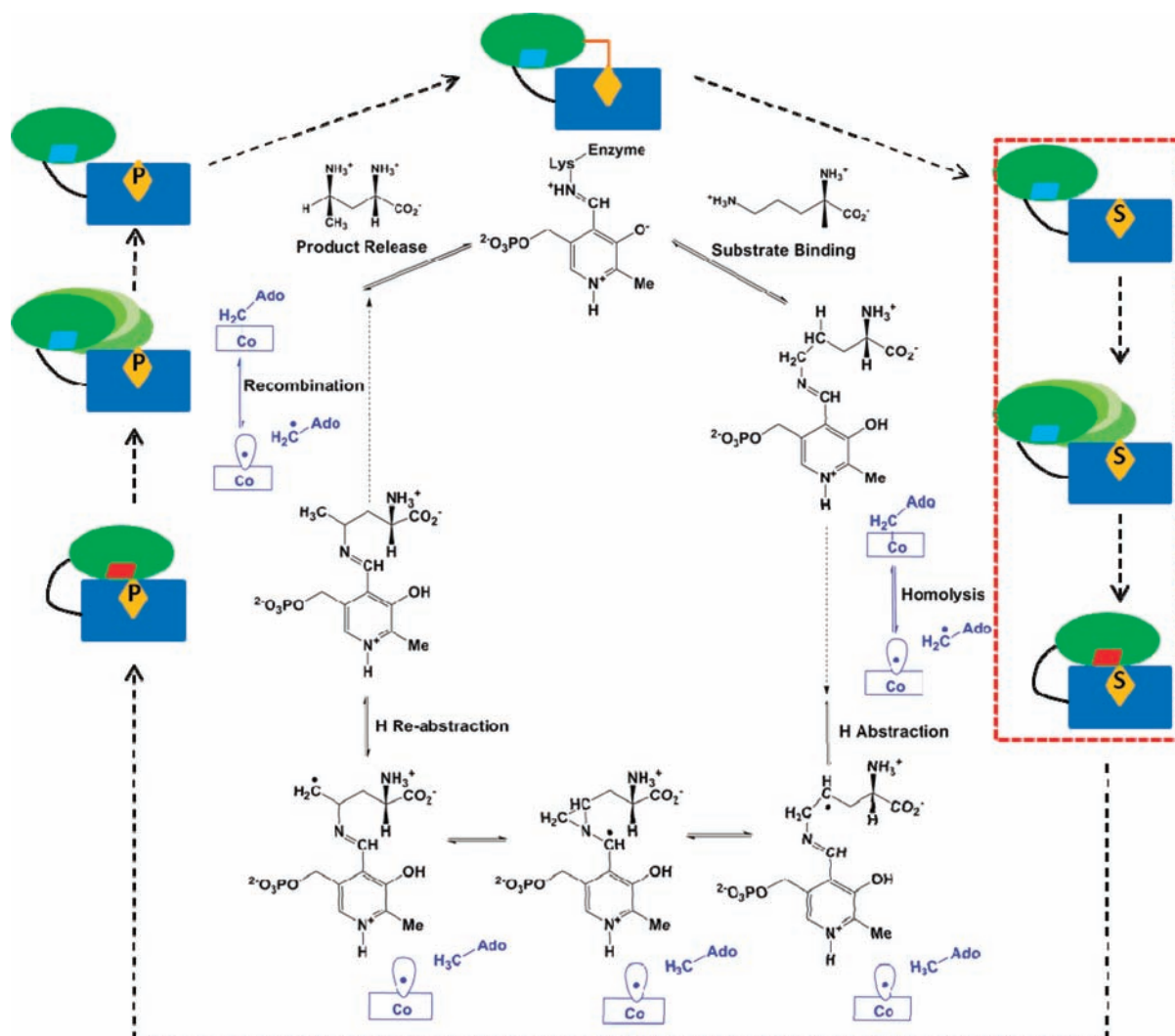
Figure 1. Coupling between the proposed reaction mechanism and the conformational rearrangement of the Rossmann domain (adapted from ref 26). (1) The inner cycle illustrates the proposed reaction mechanism. (2) The outer cycle illustrates how the conformational rearrangement of the Rossmann domain is coupled to the chemical steps. TIM-barrel domain: blue rectangular box; the Rossmann domain: green circle; AdoCbl: light blue parallelogram when the Co−C bond is intact and red when the Co−C bond is activated; PLP cofactor: yellow diamond. In the resting state (top figure), the Rossmann domain is located ∼23 Å from the 5′-deoxyadenosyl moiety of AdoCbl. This configuration is maintained through an internal aldimine link (orange line) between Lys 629 and PLP. Substrate binding has been proposed to displace Lys629 to form an external aldimine link between the substrate and PLP. This effectively "frees" the Rossmann domain so that it can reach the closed form. Once in the closed form, the chemical steps in the catalytic cycle (homolysis, H abstraction, radical-based isomerization, and recombination) occur to form the product-bound PLP. Following product release, the internal aldimine link is reformed and the enzyme returns to the resting state. (3) The red rectangular box with dashed line indicates the conformational rearrangement and catalytic step that have been studied in this work.

The $\alpha_2\beta_2$ heterodimeric structure of OAM comprises two subunits (Figure 2A; the two active sites are referred to as A and B throughout this paper). The larger β subunit comprises a TIM-barrel dimerization domain (TD) and a Rossmann-like domain (RD). The smaller α subunit comprises an extended α-helix followed by a four-helical knot. This forms an "accessory clamp" wrapping around the sides of the TIM-barrel the function of which is currently unknown.[23] The $\alpha_2\beta_2$ heterodimer undergoes a domain swap, where the Rossmann domain of one β subunit interacts with the TIM-barrel domain of the other β subunit. A 15-residue long loop connects the Rossmann and TIM-barrel domains. Despite the lack of overall sequence homology, OAM exhibits a striking resemblance at the three-dimensional level to class-I isomerases, for example, methylmalonyl-CoA mutase (MMCM)[24] and glutamate mutase (GM).[25] The AdoCbl-binding domains of all three enzymes have a

Rossmann-like fold and their substrate-binding domain a TIM-barrel motif.

Recently determined crystal structures of OAM[26] reveal that the Rossmann domain is tilted toward the edge of the TIM barrel domain in the resting state and is thus distant from the enzyme active site. This "edge-on" conformation introduces a distance of ∼25 Å between the 5′-deoxyadenosyl (Ado) moiety of AdoCbl and the PLP-bound substrate. This conformation is inconsistent with Co−C bond homolysis, hydrogen abstraction from the substrate, and further radical propagation. This is in sharp contrast to the structures of MMCM and GM where the Rossmann domain is positioned directly above the TIM-barrel ("top-on"), a configuration that positions the Ado group within ∼7 Å of the bound substrate. The crystallographic study of OAM[26] further indicates that the Rossmann domain could reach a "closed" conformation within the confines of the crystal
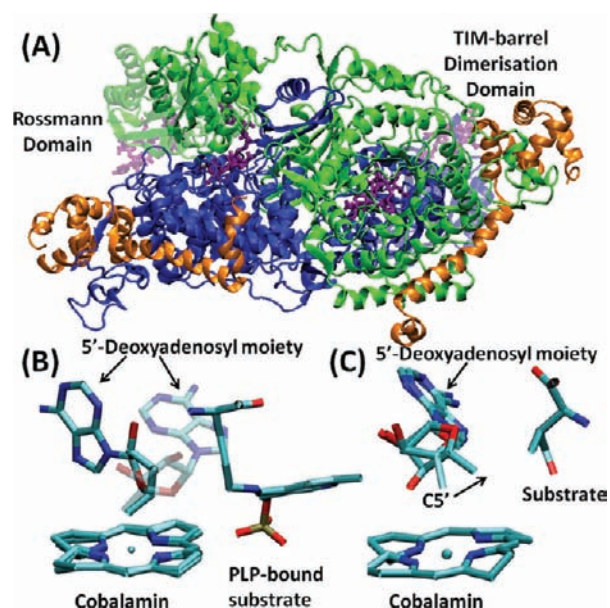
Figure 2. (A) Structure of OAM (PDB code: 3KOZ). The Rossmann-like domain and the TIM-barrel dimerization domain of the two subunits are colored in green and blue, respectively. The accessory clamp is displayed in orange. Cofactor AdoCbl is displayed as purple sticks. The open conformation of the Rossmann domain is shown in transparent green whereas the closed conformation is shown in solid green. (B) The two conformations of the 5′-deoxyadenosyl (Ado) moiety of AdoCbl in the open form (transparent line) and in the closed form (solid line). (C) The ribose is crystallized in two conformations in glutamate mutase (PDB code: 1I9C). C5′ is shown in two slightly altered orientations.

lattice in which the homolytic rupture of the Co−C bond could occur. This is reinforced by EPR spectroscopic studies[27] which suggest a distance of ~6 Å between the two paramagnetic centers (Co^{2+} and the organic radical intermediates derived from the PLP-bound substrate, Figure 1) during the intermediate steps of the catalytic cycle. Nevertheless, a crystal structure of OAM in this closed form could not be captured, probably a consequence of the equilibrium between the open and closed forms being poised toward the open form.

While structural and experimental evidence has provided insight into this essential domain conformational rearrangement that occurs during the catalytic cycle of OAM (Figure 1), a detailed understanding of how it is coupled to the activation of the Co−C bond is needed. The Co−C bond cleavage and catalytic origin in other AdoCbl-dependent enzymes have been studied by several high-level combined quantum mechanics and molecular mechanics (QM/MM) calculations.[7,8,28−32] Jensen et al. investigated the Co−C bond cleavage and catalytic origin in GM.[29] Warshel, Truhlar, Kozlowski, and their co-workers examined the catalytic effect, tunnelling effect, and Co−C bond cleavage in MMCM.[7,8,31] Two of the present authors have also investigated the Co−C bond homolytic cleavage and catalytic origin in MMCM by ONIOM calculations.[28,30] The transition state of the Co−C bond cleavage was located for the first time.[30] In addition, a substantial conformational change of the ribose was found to occur during the homolysis, and a stepwise mechanism for the Co−C bond cleavage and hydrogen transfer was supported in MMCM.[28,30] Combined QM/MM and ONIOM methods have been shown to be essential for understanding the Co−C bond cleavage in the AdoCbl-dependent enzymes.

In this study, we were able to model the "closed" form of OAM based on the closely related GM. By applying molecular dynamics (MD) simulations and targeted MD (TMD) simulations, we validated the modeled structure of the closed form and generated an atomistic picture of the large-scale domain conformational change in OAM. The emerging picture suggests that in going from the open form (catalytically inactive) to the closed form (catalytically active), the Rossmann domain effectively approaches the active site as a rigid body. It undergoes a three-phase combined rotational and translational movement to bring AdoCbl into the active site. This process is coupled to repositioning of the Ado moiety of AdoCbl from the eastern conformation in the open form to the northern conformation in the closed form. Combined QM/MM calculations further indicate that the Co−C bond cleavage in the open form has insignificant protein effect, rendering it unusually stable and thus catalytically inactive, while the Co−C bond is substantially weakened upon formation of the closed form. This weakened Co−C bond is mostly a consequence of the Ado group being under increased steric strain from the active site. Our computational studies present evidence that OAM may employ the Rossmann domain conformation to control the activation of the Co−C bond homolytic rupture, providing new insight into the biological control of B_{12}-dependent radical chemistry.

2. MATERIALS AND METHODS

2.1. Starting Protein Structures Setup. The calculations were based on the crystal structure of OAM with the Rossmann domain in the open form and with the cofactor AdoCbl and the PLP-bound substrate ornithine (i.e., with the external aldimine link) present in the active site (PDB code: 3KOZ). The closed form of OAM is modeled based on a related AdoCbl-dependent enzyme, glutamate mutase (GM) (PDB code: 1I9C), where a similar AdoCbl-binding Rossmann domain was directly positioned over the substrate-binding TIM-barrel. The program COOT[33] was used to superimpose the backbone of the Rossmann and TIM-barrel domains, respectively, onto their counterparts in the structure of GM using the secondary structure matching algorithm developed by Krissinel and Henrich.[34] The Rossmann domains from the two enzymes share 28% sequence identity and were superimposed with a rms deviation of 1.7 Å for the Cα atoms. The TIM-barrel domains share a sequence identity of 15% and were superimposed with a rms deviation of 2.2 Å for the Cα atoms. In instances where steric clashes occurred between the side chains of residues from the two domains, the configurations of the side chains were adjusted based on the rotamers predicted by COOT. The Ado moiety in the open form of OAM lies on top of pyrrole ring B of the cobalamin. This eastern conformation of the adenosine moiety clashes with the substrate in the modeled closed form (see Figures 1 and 2 for a description of this orientation). Reorientation to the northern conformation (the northern conformation as observed in GM was used as the template, Figure 2) places C5′ of the Ado moiety in the position consistent with a distance (~6 Å) between the radical pair suitable for direct hydrogen abstraction.[27] The side chain conformation of Glu338 in the modeled closed structure of OAM was adjusted to form hydrogen bonds with the hydroxyl group of the ribose in the Ado moiety.

2.2. MD Simulations. MD simulations of OAM were performed using AMBER9[35] with the AMBER96 force field.[36] The AMBER parameters for AdoCbl were taken from the literature.[37] The atom types and the corresponding force constants to describe the PLP-bound ornithine were assigned by analogy with similar chemical moieties. The equilibrium values for the bonds, angles, and dihedral angles were obtained by optimizing the structure at the B3LYP/6-31G* level of theory. The partial atomic charge was computed by RED[38] in conjunction with RESP implemented in AMBER9. The ionizable residues were modeled in the protonation state corresponding to pH 7 obtained using programs H++[39,40] and PROPKA.[41−43] The system, comprising 1701 amino acid residues, AdoCbl, and

PLP-bound substrate, was solvated in a rectangular water box using the TIP3P model with at least 8 Å between the edge of the box and the protein. Na^+ ions were added to neutralize the overall charge of the system. The final system contains a total of 146 613 atoms. Following minimization, the system was heated to 298 K in 20 ps with a step size of 1 fs under constant volume condition and then equilibrated for 200 ps under constant pressure condition. The production trajectories were collected for 2 ns with a step size of 2 fs under constant pressure condition for the open and closed forms, respectively.

2.3. TMD Simulations. TMD simulations[44,45] were performed by applying the following time-dependent, harmonic restraint bias to all $C\alpha$ atoms of the protein and the heavy atoms of AdoCbl and PLP-bound substrate:

$$E_{TMD} = 0.5 \times N \times k \times (Current\_RMSD - Target\_RMSD)^2$$

where N is the number of atoms included in the bias and k is the harmonic force constant. *Current_RMSD* is the rms deviation (mass weighted) between the configuration at a time point and the target configuration (*Target_RMSD*).

Since smaller force constants make the conformation transition more "natural", several benchmarking 1 ns simulations were carried out with the force constant values of 1, 3, and 5 kcal mol^{-1} Å^{-2}, respectively.[46,47] All simulations converged (i.e., approached the target structure) at the end of the simulation; therefore, force constants of 1 and 3 kcal mol^{-1} Å^{-2} were chosen to perform the production run. Two 2 ns TMD simulations were performed where the structure of OAM in the open state (equilibrated in the previous MD simulation) is gradually driven toward the structure in the closed form (equilibrated in the MD simulations) with force constants of 1 and 3 kcal mol^{-1} Å^{-2}, respectively. Three TMD simulations in the reverse direction were also performed—driving the structure of the closed form to the open form with force constants of 1 and 3 kcal mol^{-1} Å^{-2}, respectively (Table 1).

Table 1. Summary of the TMD Trajectories

direction	trajectory	force constant (kcal mol^{-1} Å^{-2})
open to closed	Traj 1	1
	Traj 2	3
closed to open	Traj 3	1
	Traj 4	3
	Traj 5^a	1

^{a}With a slightly altered initial structure.

This is to achieve better sampling of the conformational space in the transition between the two forms of OAM. The trajectories were analyzed using the PTRAJ module in AMBER9 and program DYNDOM[48−50] and VMD (http://www.ks.uiuc.edu/Research/vmd/).[51]

2.4. Active-Site Model Calculations. Two model systems were set up to investigate whether the conformation of the Ado moiety with respect to the cobalamin influences the stability of the Co−C bond. The models contain the corrin ring of cobalamin, the imidazole of His 618, and the Ado moiety (see Figure S1 in Supporting Information for more details). The Ado moiety was placed in the configuration of the open and the closed forms, respectively, in each model, as seen from the MD simulations. An angle formed between two atoms in the adenine ring and one atom in the cobalamin was constrained during the Co−C bond elongation to maintain the configuration of the Ado moiety (Figure S1 in Supporting Information). The quantum mechanical calculations of the homolytic dissociation of the Co−C bond in the model systems were carried out using the Gaussian09[52] program. The BP86 functional[53,54] and 6-31G* (5d) basis set were applied[55] for geometry optimization and evaluation of energies along the Co−C bond elongation process.

2.5. ONIOM Calculations. To study the homolytic bond dissociation energy of the Co−C bond in the open and closed forms of the enzyme, combined QM/MM calculations were carried out with a two-layer ONIOM[56,57] scheme—as implemented in Gaussian09—and mechanical embedding (ME). Since the ME scheme does not include

polarization of the MM region in the QM Hamiltonian, additional single-point calculations were carried out using the electronic embedding (EE) scheme, based on the ME-optimized geometry. The single-point EE calculations gave a potential energy profile of the Co−C bond elongation similar to that in the ME scheme (see Figure S8 in the Supporting Information). The BP86 functional, 6-31G*(5d) basis set, and the AMBER96 force field were employed to represent the QM and the MM regions, respectively. The QM region comprised 86 atoms, including the corrin ring of the cobalamin, the imidazole of His 618, and the Ado moiety (Figure 3). The MM region contained
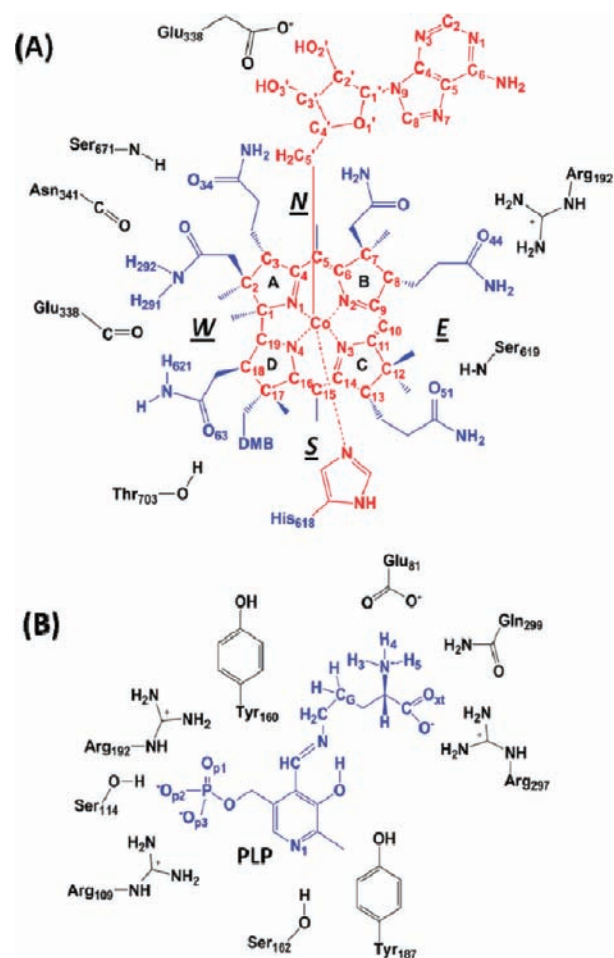

Figure 3. (A) Interactions between the active site residues and AdoCbl in the closed form. The northern (*N*), southern (*S*), western (*W*), and eastern (*E*) orientation of the 5'-deoxyadenosyl moiety refer to the vicinity of C5, C15, the C1−C19 bond, and C10, respectively, in this view of B12. The four pyrrole-like rings are labeled with A, B, C, and D to help the description of the orientation of the 5'-deoxyadenosyl moiety. Atoms in red were treated quantum-mechanically in the ONIOM calculations. (B) Interactions between the active-site residues and the PLP-bound substrate. The side-chains of Tyr160 and Tyr 187 form π−π interactions with cofactor PLP.

residues within 20 Å of the cobalt atom of AdoCbl. Residues within 15 Å of the Co atom were free to move during the geometry optimization while the rest were frozen to maintain the overall shape of the protein. The entire QM/MM system contains 3669 atoms for the open form and 8676 atoms for the closed form, respectively.

3. RESULTS AND DISCUSSION

3.1. Eastern and Northern Conformations of the Ado Moiety of AdoCbl in the Open and Closed Forms. *3.1.1. MD Simulation of the Open Form.* In the resting state of the

enzyme, the conserved Lys 629 anchors the Rossmann domain to the TIM-barrel domain of the opposite subunit through an imine link (the internal aldimine) to the PLP (see Figure 1 and figure legend), thus locking the substrate-free enzyme in the open conformation. Substrate binding displaces Lys 629 to form a new imine link between the substrate and PLP (the external aldimine). This effectively "frees" the Rossmann domain and poises it for reorienting over the TIM-barrel into the proposed closed conformation.

The MD simulation of the open form is based on the crystal structure of OAM (PDB code: 3KOZ) with the substrate bound to PLP through the external aldimine link. In the subsequent discussion, the open form referred to is always this external aldimine link structure unless otherwise specified (Figure 1). The Rossmann domain, which harbors AdoCbl, is tilted toward the edge of the PLP-binding TIM-barrel domain. This "edge-on" orientation of the Rossmann domain projects the Ado group toward the bulk solvent and ~25 Å away from the active site where the PLP-bound substrate presents; thus, AdoCbl is largely solvent-exposed in the open conformation (Figure 2). The overall structure of OAM in this open form remains stable during the 2 ns MD simulation based on the Cα RMSDs fluctuating below ~2 Å (Figure 4A).

AdoCbl-dependent enzymes can achieve rate accelerations of the Co−C homolytic rupture by 11−13 orders of magnitude.[6,58] The precise origin of this catalytic power has been discussed in terms of ground-state destabilization (a "strain" hypothesis),[28,59−62] effect of protein dynamics,[9] and transition state stabilization through electrostatic interactions.[7] In particular, it has been suggested that the protein may "pull" the ribose of the Ado group through steric and hydrogen bonding interactions, causing strain on the axis of Co−C5′−C4′, hence weakening the Co−C5′ bond substantially.[28,29,59] Since the Co−C bond in the AdoCbl-dependent enzymes is much weaker than a typical organic single bond, it is frequently crystallized in a ruptured state.[23] Interestingly, the usually labile Co−C bond is intact in the crystal structures of the open form of OAM.[26] It is also intriguing that this unusual stability of the Co−C bond is associated with the Ado group in the eastern position, a configuration not previously observed in other AdoCbl-dependent isomerases. This eastern conformation of the Ado moiety as observed in the crystal structures was maintained during the MD simulation, with the dihedral angle N3−Co−C5′−O1′ of AdoCbl fluctuated around ~60° (Figure 5).

3.1.2. MD Simulation of the Closed Form. The "top-on" closed form of OAM was constructed by superimposing the backbone of the Rossmann domain and TIM-barrel domain of the open form, respectively, onto their counterparts in the structure of GM, where a similar AdoCbl-binding Rossmann domain is directly positioned over the substrate-binding TIM barrel domain (see Materials and Methods for details). The overall structure of this modeled closed form is stable throughout the 2 ns simulation with the Cα RMSDs below 2 Å (Figure 4A). The structures of the closed form, in particular the TIM-barrel domain, exhibit reduced Cα RMSFs over the course of the MD simulation, compared to those in the MD simulation of the open form (Figure 4B). The decreased overall RMSDs and RMSFs indicate that the domain conformational rearrangement into the closed form may bring the enzyme into a tighter packing state with reduced global flexibility.

In contrast to the open form where AdoCbl is largely solvent exposed, the Rossmann domain in the closed form is docked directly above the TIM-barrel in the closed form, shielding
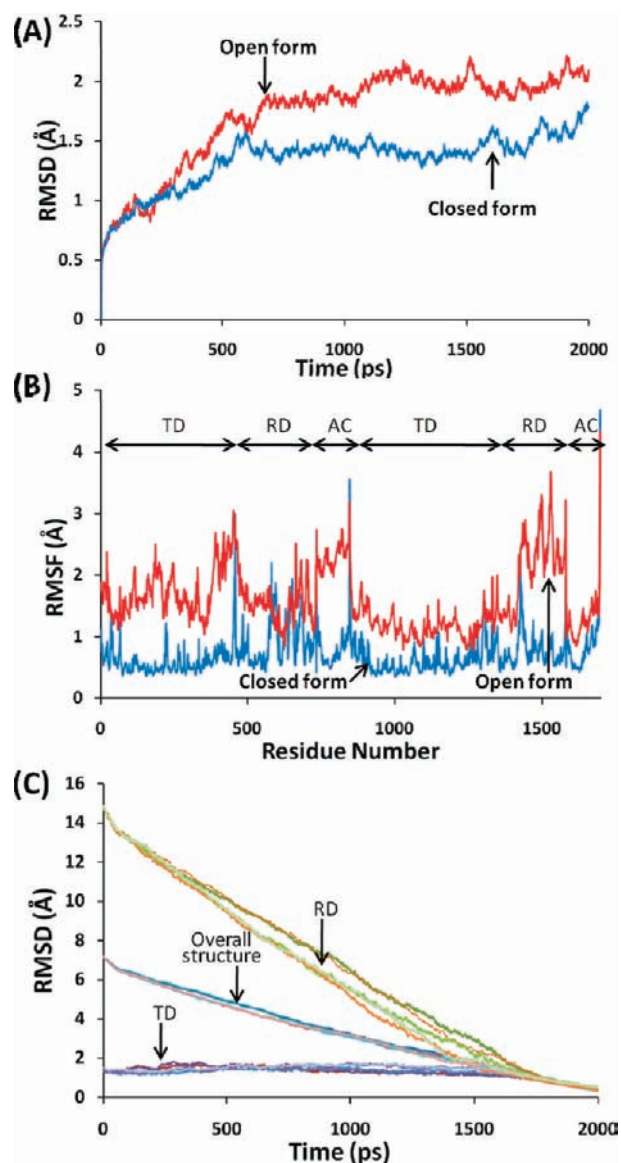

Figure 4. (A) RMSDs of the Cα atoms during the MD simulations of the open form (red line) and the closed form (blue line). (B) RMSFs of the Cα atoms over the MD simulations of the open form (red line) and the closed form (blue line). The TIM-barrel dimerization domain (TD), the Rossmann domain (RD), and the accessory clamp (AC) are labeled, respectively. (C) RMSDs of the Cα atoms in the Rossmann domain (RD), the TIM-barrel domain (TD), and the overall structure during the five independent sets of TMD simulations (measured following the superimposition of the TD).

AdoCbl from bulk solvent. Compared to the open form, the cobalamin is seen to have rotated by ~10° and moved by ~1 Å in terms of its position of binding to the Rossmann domain. Several new interactions are formed in the closed form to tighten the binding of AdoCbl, mainly between the peripheral propionamide and acetamide groups attached to the corrin ring and the active-site residues Arg 192, Glu 338, Asn 341, Ser 619, Ser 671, and Thr 703 (Figure 3A). On the other hand, multiple interactions, including hydrogen bonds and π−π interactions, serve to lock the PLP-bound substrate at the active site of OAM (Figure 3B). These interactions exhibit small fluctuations (Table S1 in Supporting Information), indicating an active site that is structurally stable. This is consistent with what is
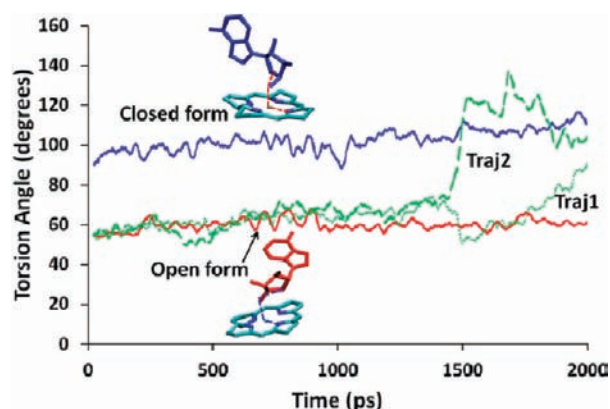
Figure 5. Dihedral angle N3−Co−C5′−O1′ during the MD simulation of the open form (red line), closed form (blue line), and TMD simulations of traj 1 (green dotted line) and traj 2 (green dashed line).

observed in MMCM and GM, where extensive interactions between the substrate and active site residues have been suggested to assist in stabilizing the reactive radical intermediates and prevent their diffusive escape.[6,63]

The Ado moiety has to be repositioned from the eastern conformation in the open form to the northern conformation to avoid steric clashes with the active-site cavity in the closed form (Figures 1 and 2). This places C5′ of the Ado moiety in a position suitable for direct hydrogen abstraction from the substrate (∼6−7 Å) during the catalytic cycle.[27] The hydrogen bond formed between Glu 338 and the hydroxyl group of the ribose, conserved in several AdoCbl-dependent enzymes, is also maintained in the closed form. This hydrogen bond and the steric constraint of the active site help maintain the northern conformation of the Ado moiety with the dihedral angle N3−Co−C5′−O1′ of AdoCbl fluctuating around ∼100° during the simulation of the closed form (Figure 5).

3.2. Ado Group Conformational Switch from Eastern to Northern Is Coupled to the Protein Domain Conformational Change. To probe the pathway of the Rossmann domain conformational transformation between the open and the closed forms, a series of TMD simulations were performed. To access the type of motions which usually occur on a micro- to millisecond time scale, the most rigorous simulation methods, such as umbrella sampling, require an energetic bias to be applied along a well-defined reaction coordinate. Since our knowledge of the process of OAM's domain conformational change at the atomic level is very limited, it is difficult to predefine a reasonable reaction coordinate in the dimensional space occupied by the enzyme. Although algorithms[64] have been developed to improve the generation of independent trajectories without previously defining a reaction coordinate, the sheer size of OAM (∼1700 residues) and its structural complexity prevent the study of the proposed transition path by more computationally expensive approaches. On the other hand, TMD applies the energetic bias that decreases the rmsd between the moving structure and the target structure, providing the qualitative characteristics of the conformation transition path.[46,65−68] Although TMD is not guaranteed to follow the minimum free energy path, we generated several series of trajectories each with slightly altered initial conditions to achieve better sampling of the conformational space during the transition.

In total five 2 ns TMD simulations were performed (see Material and Methods and Table 1). Figure 4C shows the

Cα RMSDs of the overall structure, the Rossmann domain, and the TIM-barrel domain, respectively, as a function of the progress of the conformational change. The initial rmsd of the Rossmann domain between the open and the closed forms is ∼14 Å (following superimposition of the respective TIM-barrel dimerization domains). As the TMD simulation progresses, the Cα RMSDs of the Rossmann domain decreases smoothly from ∼14 Å to 0.5 Å while the Cα RMSDs of the TIM-barrel domain remain close to the starting value of ∼1.5 Å. Furthermore, the Cα RMSDs within the Rossmann domain remain below 1.2 Å along the simulation trajectories (data not shown). These rmsd plots illustrate that the Rossmann domain is effectively approaching the TIM-barrel as a rigid body.

This rigid body movement of the Rossmann domain is defined by the program DYNDOM as a combination of a ∼52° rotation and a ∼14 Å translation. Snapshots saved every 200 ps of the TMD trajectories were further analyzed by DYNDOM to provide a qualitative description of the transformation path (Figure 6 and Figure S3 in the Supporting Information). As expected, the Rossmann domains of the two respective subunits cover similar paths within one TMD trajectory. This is demonstrated by the overall similarity between Figure S3(A) and S3(B) in the Supporting Information. On the other hand, the paths the Rossmann domain follows depend to some extent on the direction of the simulation. When pulling the structure from the open form to the closed form (Traj 1 and 2), the movement of the Rossmann domain follows an approximate three-stage process, while when the conformational transition is sampled from the closed form toward the targeted open form (Traj 3, 4, and 5), the transition path (analyzed using the open form as the reference and in the direction from the open form to the closed form) can be seen as a smooth curve with two phases (Figure 6A).

Figure 6B provides a pictorial representation of the pathway of the domain conformational rearrangement. Structures were chosen to highlight the rotational/translational movement of the Rossmann domain during the TMD simulations, as indicated by Figure 6A. Close examination of these structures reveals that a ∼30° rotation of the Rossmann domain is required to bring the AdoCbl from the edge of the TIM-barrel domain to the proximity of the active site. To overcome a "barrier" formed by a loop region (residues 110−128) of the TIM-barrel domain that impedes access into the active-site cavity (Figure 6C), a sequential translation−rotation is observed, involving first a translation of ∼12−14 Å with a subsequent ∼15−20° rotational movement of the Rossmann domain. When moving away from the active-site cavity (in the reverse direction − from the closed form to the open form), these rotational and translational movements are concerted. This seems to indicate that the transition path is not only dependent on the perturbation force but also dependent on the ease of the motions of atoms that are induced by the perturbation force, consistent with a previous study by Post and co-workers.[68]

The adenine portion of the Ado moiety lies above the B ring of the cobalamin (the eastern conformation) in the open form with a torsion angle N3−Co−C5′−O1′ of ∼60° (Figure 5). Upon forming the closed form, it is positioned roughly perpendicular to the cobalamin, lying over the A ring of the cobalamin (northern conformation) with a torsion angle N3−Co−C5′−O1′ of ∼100° (Figure 5). This conformational switch leads to a tilting of the ribose to a position similar to that seen in the active site of GM (Figure 2). TMD simulations indicate that this conformational switch of the Ado moiety only occurs
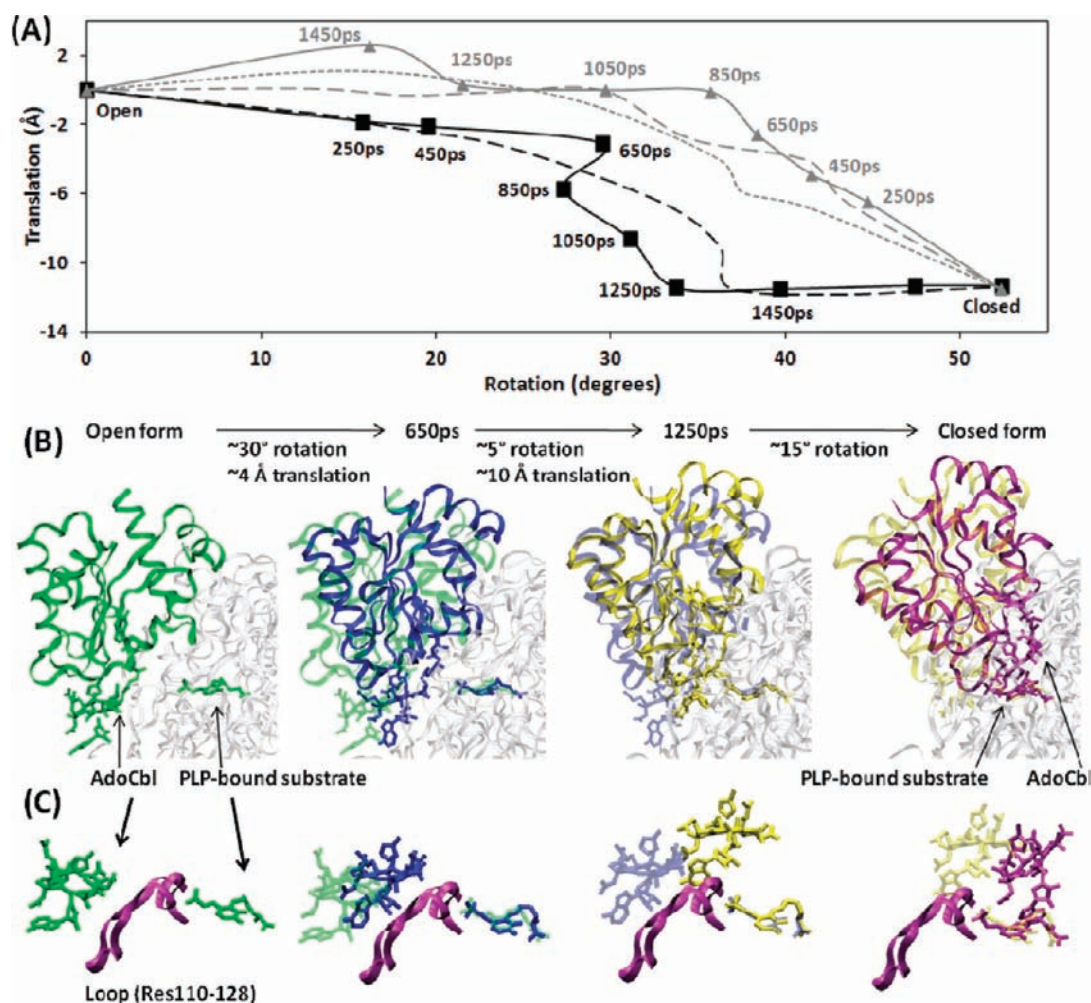
Figure 6. Atomic description of the conformational rearrangement of the Rossmann domain. (A) The transition path as defined by the overall rotation and translation of the Rossmann domain to the TIM barrel domain (Traj 1: solid black line, Traj 2: dashed black, Traj 3: solid gray, Traj 4: dashed gray, Traj 5: dotted gray). (B) Snapshots along the trajectories (with the TMD simulation time labeled) are selected to highlight the rotational and translational movement in Traj 1. (C) Close-up of the cobalamin ring and PLP-bound substrate within each snapshot in panel B. The loop formed by residues 110−128 that "gates" the active-site cavity is displayed in purple ribbon.

at the later stage of the Rossmann domain conformational rearrangement (Figure 6) when it predominantly engages in rotational movement to adjust to the cavity of the active site (after 1.5 ns of TMD simulations of Traj 1 and 2); that is, the steric constraint of the active site "forces" the Ado group to rotate into the northern conformation. Glu 338 from the TIM barrel domain, which is more than 20 Å away in the open form, subsequently forms a hydrogen bond with the hydroxyl group of the ribose ring, hence further stabilizing its configuration.

3.3. Possible Activation Mechanism of the Co−C Bond in OAM. An early computational study shows that rotation of the torsion angles centered on the Co−C5′ bond in the gas phase results in four conformations (northern, southern, western, and eastern) of the Ado moiety that occupy local minima.[37,69] These conformations are separated by relatively low energy barriers (less than 10 kcal/mol) caused by straining the Ado group to various degrees. The northern conformation is the position the Ado group adapts in the modeled closed form of OAM and in the crystal structures of GM and MMCM while a two-dimensional NMR study indicated that free AdoCbl fluctuates between the eastern form and the southern

form. This raises the question: Is it the peculiar eastern configuration of the Ado group or is it the solvent exposure of AdoCbl and the lack of steric strain from the protein environment that gives rise to the unusual stability of the Co−C bond in the catalytically inactive open form? Also, what are the factors that serve to activate the Co−C bond when the conformation of the Ado moiety switches from the eastern to the northern position driven by the Rossmann domain conformational rearrangement? To answer these questions, the Co−C bond homolytic rupture in the gas phase and in OAM was studied by DFT and ONIOM type QM/MM calculations.

3.3.1. Co−C Bond Homolytic Rupture in the Model Systems. To investigate whether the conformation of the Ado moiety of AdoCbl, in particular the eastern and northern conformations with respect to the cobalamin ring, influences the bond dissociation energy (BDE) of the Co−C bond, a model system was employed. The model contains the corrin ring of the cobalamin, the imidazole ring of His 618, and the Ado moiety. Such a structural model has been demonstrated as being sufficient to describe Co−C bond homolysis.[31] The Co−C BDE is calculated to be 27.8 kcal/mol (without zero-point energy [ZPE])

when the Ado moiety is in the eastern conformation (the open form) (Figure 7 and Figure S1 in Supporting Information). When the Ado moiety is positioned in the northern conformation (the closed form), the BDE of the Co−C bond is increased to 33.0 kcal/mol (without ZPE) (Figure 7 and Figure S1 in Supporting Information), consistent with the experimental measurement[70] and the calculated BDE from several other computational studies on model systems in this conformation.[28,29,31] These calculations of the model systems demonstrate that distortion of the ribose through varying conformation of the adenine portion could influence the stability of the Co−C bond by ∼5 kcal/mol. Nonetheless, the conformation of the Ado group alone is not sufficient to explain the unusual stability of the Co−C bond in the catalytically inactive open form.

3.3.2. Co−C Bond Homolytic Rupture in the Enzyme. The dissociation of Co−C bond in the enzyme was studied with an ONIOM-type approach. The BDE of the Co−C bond in the open conformation of OAM is calculated to be 26.5 kcal/mol (Figure 7 and Figure S8 in the Supporting Information), almost identical to that in the gas phase. In contrast, the potential energy surface (PES) of the elongating Co−C bond in the closed conformation of OAM differs significantly from that in the gas phase. The homolytic rupture of the Co−C bond takes place with a transition state at the Co−C distance of 2.8 Å and a barrier height of 10.9 kcal/mol (Figure 7 and Figure S8 in the Supporting Information). Frequency calculations confirm that the imaginary frequency of this transition state corresponds to the breaking of the Co−C bond. The reaction energy between the reactant (Co−C distance ∼2.0 Å) and the product (Co−C distance ∼3.8 Å) is reduced to 2 kcal/mol, compared to that of 33.0 kcal/mol in the gas phase. This BDE profile of the closed form compares particularly well with a previous computational study[30] of the Co−C homolytic rupture catalyzed by MMCM that gives a barrier height of ∼10 kcal and reaction energy of ∼2.5 kcal/mol. Our results are also in good agreement with several other previous computational studies of GM and MMCM.[28,29] In addition, the ONIOM-optimized Co−C bond is 2.05 Å in the closed form, 0.03 Å longer than that in the open form (Table 2). A 0.03 Å longer Co−C bond could partially account for ∼5 kcal/mol decrease in BDE. The longer and

Table 2. Structural Parameters of AdoCbl during the Co−C Bond Elongation in ONIOM Calculations (bond lengths in Å; angles and dihedral angles in deg)[a]

	open form		closed form		
	R	P	R	TS	P
Co−C5′	2.02	3.8	2.05	2.8	3.8
Co−N$_{His618}$	2.22	2.08	2.22	2.2	2.15
Co−C5′−C4′	130.7	122.5	134.3	132.1	112.9
N3−Co−C5′−O1′	24.6	44.5	−74.9	−142.5	−154.6
N3−Co−C5′−C4′	3.6	44.9	−71.7	−92.3	−115.7
O1′−C1′−N9−C8	−87.8	−97.7	32.5	44.8	58.7
C1′−C2′−C3′−C4′	−1.5	2.7	34.1	33.2	29.9

[a]The dihedral angle O1′−C1′−N9−C8 describes the adenine plane relative to the ribose, and the dihedral angle C1′−C2′−C3′−C4′ describes the puckering of ribose. R stands for reactant, P for product, and TS for transition state.

weakened Co−C bond in AdoCbl in comparison to MeCbl has been attributed to the intrinsic steric and electrostatic effects of the Ado group.[71]

Raman spectroscopy studies indicate that in MMCM, the Co-Ado axis is tilted to a small extent in the resting enzyme and to a larger extent in the substrate-bound state, suggesting that the steric change is a contributor to activation of the Co−C bond.[59] Recent computational studies have provided evidence to further indicate the effect of distortion of the ribose by the protein environment on the energetics and geometry of the Co−C bond cleavage in GM[29,32] and MMCM.[28] To pinpoint the factors that give rise to the distinct energetics of the Co−C bond homolytic rupture in the open and closed forms, the geometrical features that define the position of ribose relative to the cobalt atom and the corrin ring were compared (Table 2, see Figure 3 for atoms names). The ribose in the open form is almost planar, as indicated by the dihedral angle C1′−C2′−C3′−C4′[72,73] while formation of the closed form puckers the ribose by ∼34°. Furthermore, the energy cost for the structural distortion (the "strain" energy) of the whole QM region (His + Corrin + Ribose + Adenine) in the open form and the closed form was evaluated, respectively. This was done by comparing the energy difference of each part optimized in the enzyme and
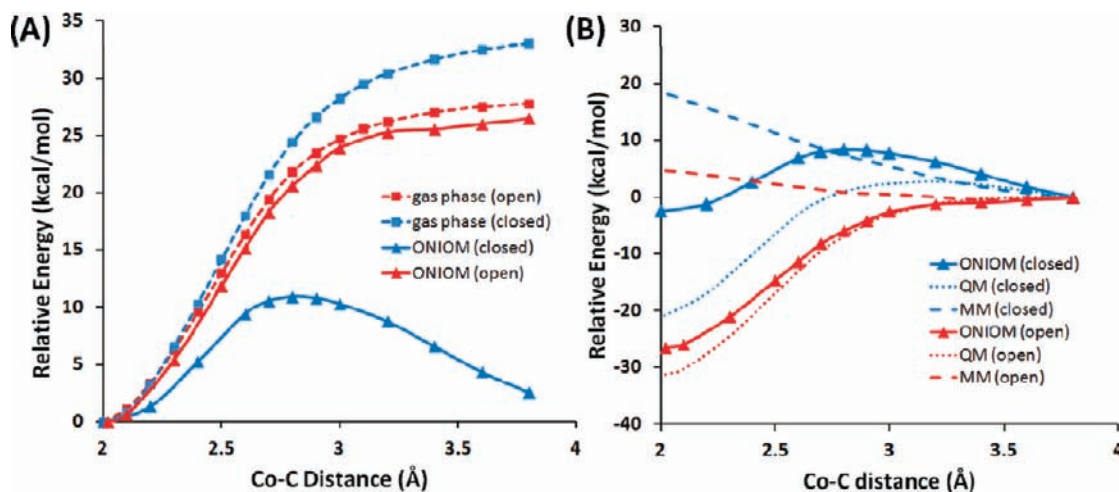

Figure 7. (A) Potential energy profiles of the Co−C bond homolytic rupture in the gas phase (dashed line) and in the ONIOM (QM/MM) approach (solid line) for the open form and the closed form. The energies are given relative to the reactant where the Co−C bond is intact. (B) The QM and MM energy contribution to the overall QM/MM energy for the open and closed forms. The energies are given relative to the product where the Co−C bond is separated by 3.8 Å.

in the gas phase.[28,29] It is worth noting that the strain energy discussed here is qualitative and the strain energy evaluated for each part of the QM region is slightly coupled to one another. Remarkably, the overall QM region is subjected to substantially increased strain energy in the closed form compared to in the open form (44.6 vs21.1 kcal/mol) (Table 3) This significant

Table 3. Strain Energies (kcal/mol) for Various Parts of the QM Region

	open	closed
His + Corrin + Ribose + Adenine	21.1	44.6
Ribose + Adenine	11.3	27.1
Ribose	1.0	2.6
Adenine	5.3	4.5
Corrin	9.7	14.8

increase in the strain energy of the closed form arises predominantly from the more "strained" Ado moiety (27.1 vs 11.3 kcal/mol) and to a lesser extent the corrin ring (14.8 vs 9.7 kcal/mol).

The protein effect (MM energy component of the combined QM/MM ME energy) on the homolytic rupture of the Co−C bond in the open form is just ~4.7 kcal/mol, significantly less than that of ~18.6 kcal/mol in the closed form (Figure 7B). Furthermore, as shown in Figure S9 in the Supporting Information, the electrostatic (Coulomb) and van der Waals terms make the predominant contribution (7.4 kcal/mol and 8.7 kcal/mol, respectively) to the overall protein effect in the closed form. In contrast, these two terms nearly counterbalance each other in the open form, leading to the significantly reduced protein effect. Thus, the distinct energetics of the Co−C bond homolytic rupture in the closed form compared to that in the open form could be interpreted as the synergy of steric and electrostatic effects arising from tighter interactions with the surrounding enzyme.

When the Co−C bond is elongated, substantial repositioning of the adenine ring of the Ado group occurs in the open form, resembling that observed in MMCM,[30] while it remains fixed in the closed form, similar to GM[25] (Figure 8). In the closed form,
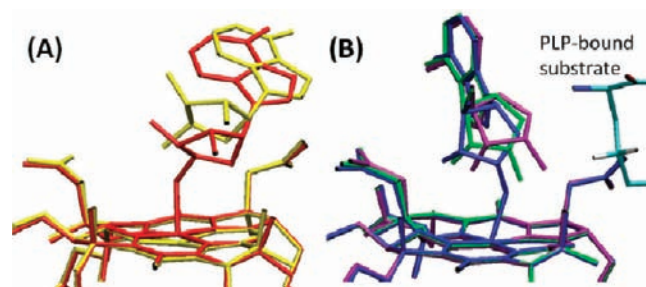

Figure 8. (A) Overlay of the structures of the reactant (red) and product (yellow) during elongation of the Co−C bond in the open form. (B) Overlay of the structures of the reactant (blue), transition state (green), and product (purple) in the closed form. For clarity, only hydrogen atoms involved in the subsequent H abstraction step are displayed. See Table 2 for geometrical features associated with these structures.

the gradual rotation of the ribose concomitant with the Co−C bond elongation positions the newly formed C5′ radical toward the PLP-bound substrate. The distance between the C5′ radical and the hydrogen it abstracts decreases from ~4.2 Å in the reactant to ~2.4 Å in the product. Figure 8B displays part of the
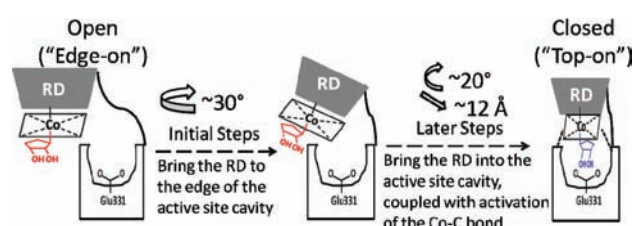

Figure 9. Schematic illustration of the large-scale domain conformational change (RD: Rossmann-like domain). The closed form is stabilized by additional hydrogen bonds between the active site residues and AdoCbl (illustrated by dashed lines) and forming a hydrogen bond between Glu 331 and the ribose of AdoCbl. The ribose color change from red to blue indicates its conformational switch from eastern to northern.

PLP-bound substrate to illustrate this change. Clearly, the position of the ribose is finely tuned in the closed form to facilitate the subsequent catalytic steps.

4. CONCLUSION

In OAM, the "edge-on" conformation of the Rossmann domain embodies a locking mechanism in which AdoCbl is kept away from the active site in the absence of the substrate. Because AdoCbl is largely solvent exposed in this open form, the Ado group lies in the eastern position, and one of the two conformations free AdoCbl adapts. The catalytically inactive form of the Co−C bond (BDE 26.5 kcal/mol) in this open conformation is not the consequence of the Ado group in the eastern position. Rather, it is the result of the Ado group being solvent exposed, thus experiencing negligible influence from the protein environment. In going from the open form to the closed form, the Rossmann domain engages initially in rotational motion, followed by translational motion, to bring the AdoCbl into the active-site cavity, thereby overcoming the steric hindrance of the loop comprising residues 110−128 (Figure 9). Formation of the "top-on" closed form between the Rossmann domain and the active-site cavity drives the Ado moiety of AdoCbl into the northern configuration where the Co−C bond is activated through the synergy of steric and electrostatic effects arising from tighter interactions with the surrounding enzyme. The protein effect (MM energy component of the overall combined QM/MM energy) on the Co−C bond increases substantially from 4.4 kcal/mol in the open form to ~16 kcal/mol in the closed form, leading to a 0.03 Å longer Co−C bond and a more distorted Ado group. This is indicated by a ~30° increase in ribose puckering and ~15 kcal/mol increase in the "strain" energy that the Ado group experiences in the closed form. Consequently, the BDE of the Co−C bond is significantly reduced to 2 kcal/mol via a transition state of 10.9 kcal/mol barrier, rendering the subsequent chemical steps feasible. In addition to OAM, at least one other AdoCbl-dependent enzyme, lysine 5,6-aminomutase (LAM), has also been proposed to adapt a similar large-scale domain rearrangement to orchestrate radical formation.[23,74] More generally, there is an increasing body of evidence that large-scale conformational change is critical for biomolecular function.[1,75] The present computational study of OAM reveals novel strategies employed by AdoCbl-dependent enzymes in the control of radical catalysis.

■ AUTHOR INFORMATION

Corresponding Author

j.pang@gre.ac.uk; mike.sutcliffe@manchester.ac.uk

Present Address

†School of Science, University of Greenwich, Medway Campus, Central Avenue, Chatham Maritime, Kent, ME4 4TB, United Kingdom.

■ REFERENCES

(1) Henzler-Wildman, K. A.; Lei, M.; Thai, V.; Kerns, S. J.; Karplus, M.; Kern, D. *Nature* **2007**, *450*, 913.

(2) Boehr, D. D.; Dyson, H. J.; Wright, P. E. *Chem. Rev.* **2006**, *106*, 3055.

(3) Kern, D.; Zuiderweg, E. R. P. *Curr. Opin. Struct. Biol.* **2003**, *13*, 748.

(4) Elber, R. *Curr. Opin. Struct. Biol.* **2011**, *21*, 167.

(5) Abeles, R. H.; Dolphin, D. *Acc. Chem. Res.* **1976**, *9*, 114.

(6) Banerjee, R. *Chem. Rev.* **2003**, *103*, 2083.

(7) Sharma, P. K.; Chu, Z. T.; Olsson, M. H. M.; Warshel, A. *Proc. Natl. Acad. Sci. U.S.A.* **2007**, *104*, 9661.

(8) Dybala-Defratyka, A.; Paneth, P.; Banerjee, R.; Truhlar, D. G. *Proc. Natl. Acad. Sci. U.S.A.* **2007**, *104*, 10774.

(9) Jones, A. R.; Hardman, S. J. O.; Hay, S.; Scrutton, N. S. *Angew. Chem., Int. Ed.* **2011**, *50*, 10843.

(10) Robertson, W. D.; Wang, M.; Warncke, K. *J. Am. Chem. Soc.* **2011**, *133*, 6968.

(11) Gruber, K.; Puffer, B.; Krautler, B. *Chem. Soc. Rev.* **2011**, *40*, 4346.

(12) Dybała-Defratyka, A.; Paneth, P. *J. Inorg. Biochem.* **2001**, *86*, 681.

(13) Zhu, C.; Warncke, K. *J. Am. Chem. Soc.* **2010**, *132*, 9610.

(14) Sandala, G. M.; Smith, D. M.; Radom, L. *Acc. Chem. Res.* **2010**, *43*, 642.

(15) Kozlowski, P. M.; Kamachi, T.; Kumar, M.; Nakayama, T.; Yoshizawa, K. *J. Phys. Chem. B* **2010**, *114*, 5928.

(16) Banerjee, R.; Dybala-Defratyka, A.; Paneth, P. *Philos. Trans. R. Soc. London, Series B* **2006**, *361*, 1333.

(17) Kamachi, T.; Toraya, T.; Yoshizawa, K. *J. Am. Chem. Soc.* **2004**, *126*, 16207.

(18) Toraya, T. *Chem. Rev.* **2003**, *103*, 2095.

(19) Barker, H. A. *Annu. Rev. Biochem.* **1981**, *50*, 23.

(20) Chen, H.-P.; Wu, S.-H.; Lin, Y.-L.; Chen, C.-M.; Tsay, S.-S. *J. Biol. Chem.* **2001**, *276*, 44744.

(21) Makins, C.; Miros, F. N.; Scrutton, N. S.; Wolthers, K. R. *Bioorg. Chem.* **2012**, *40*, 39.

(22) Wetmore, S. D.; Smith, D. M.; Radom, L. *J. Am. Chem. Soc.* **2001**, *123*, 8678.

(23) Berkovitch, F.; Behshad, E.; Tang, K.-H.; Enns, E. A.; Frey, P. A.; Drennan, C. L. *Proc. Natl. Acad. Sci. U.S.A.* **2004**, *101*, 15870.

(24) Mancia, F.; Evans, P. R. *Structure* **1998**, *6*, 711.

(25) Gruber, K.; Reitzer, R.; Kratky, C. *Angew. Chem., Int. Ed.* **2001**, *40*, 3377.

(26) Wolthers, K. R.; Levy, C.; Scrutton, N. S.; Leys, D. *J. Biol. Chem.* **2010**, *285*, 13942.

(27) Wolthers, K. R.; Rigby, S. E. J.; Scrutton, N. S. *J. Biol. Chem.* **2008**, *283*, 34615.

(28) Li, X.; Chung, L. W.; Paneth, P.; Morokuma, K. *J. Am. Chem. Soc.* **2009**, *131*, 5115.

(29) Jensen, K. P.; Ryde, U. *J. Am. Chem. Soc.* **2005**, *127*, 9117.

(30) Kwiecien, R. A.; Khavrutskii, I. V.; Musaev, D. G.; Morokuma, K.; Banerjee, R.; Paneth, P. *J. Am. Chem. Soc.* **2006**, *128*, 1287.

(31) Kozlowski, P. M.; Kamachi, T.; Toraya, T.; Yoshizawa, K. *Angew. Chem., Int. Ed.* **2007**, *46*, 980.

(32) Durbeej, B.; Sandala, G. M.; Bucher, D.; Smith, D. M.; Radom, L. *Chem.—Eur. J.* **2009**, *15*, 8578.

(33) Emsley, P.; Lohkamp, B.; Scott, W. G.; Cowtan, K. *Acta Crystallogr., Sect. D: Biol. Crystallogr.* **2010**, *66*, 486.

(34) Krissinel, E.; Henrich, K. *Acta Crystallogr., Sect. D: Biol. Crystallogr.* **2004**, *60*, 2256.

(35) Case, D. A.; Cheatham, T. E.; Darden, T.; Gohlke, H.; Luo, R.; Merz, K. M.; Onufriev, A.; Simmerling, C.; Wang, B.; Woods, R. J. *J. Comput. Chem.* **2005**, *26*, 1668.

(36) Cornell, W. D.; Cieplak, P.; Bayly, C. I.; Gould, I. R.; Merz, K. M.; Ferguson, D. M.; Spellmeyer, D. C.; Fox, T.; Caldwell, J. W.; Kollman, P. A. *J. Am. Chem. Soc.* **1995**, *117*, 5179.

(37) Marques, H. M.; Ngoma, B.; Egan, T. J.; Brown, K. L. *J. Mol. Struct.* **2001**, *561*, 71.

(38) Dupradeau, F.-Y.; Cézard, C.; Lelong, R.; Stanislawiak, É.; Pêcher, J.; Delepine, J. C.; Cieplak, P. *Nucleic Acids Res.* **2008**, *36*, D360.

(39) Gordon, J. C.; Myers, J. B.; Folta, T.; Shoja, V.; Heath, L. S.; Onufriev, A. *Nucleic Acids Res.* **2005**, *33*, W368.

(40) Anandakrishnan, R.; Onufriev, A. *J. Comput. Biol.* **2008**, *15*, 165.

(41) Li, H.; Robertson, A. D.; Jensen, J. H. *Proteins: Struct., Funct., Bioinf.* **2005**, *61*, 704.

(42) Bas, D. C.; Rogers, D. M.; Jensen, J. H. *Proteins: Struct., Funct., Bioinf.* **2008**, *73*, 765.

(43) Olsson, M. H. M.; Søndergaard, C. R.; Rostkowski, M.; Jensen, J. H. *J. Chem. Theory Comput.* **2011**, *7*, 525.

(44) Schlitter, J.; Engels, M.; Kruger, P.; Jacoby, E.; Wollmer, A. *Mol. Simul.* **1993**, *10*, 291.

(45) Schlitter, J.; Engels, M.; Kruger, P. *J. Mol. Graphics* **1994**, *12*, 84.

(46) Swift, R. V.; McCammon, J. A. *Biochemistry* **2008**, *47*, 4102.

(47) Weng, J.-W.; Fan, K.-N.; Wang, W.-N. *J. Biol. Chem.* **2010**, *285*, 3053.

(48) Hayward, S.; Kitao, A.; Berendsen, H. J. C. *Proteins: Struct., Funct., Bioinf.* **1997**, *27*, 425.

(49) Hayward, S.; Berendsen, H. J. C. *Proteins: Struct., Funct., Bioinf.* **1998**, *30*, 144.

(50) Poornam, G. P.; Matsumoto, A.; Ishida, H.; Hayward, S. *Proteins: Struct., Funct., Bioinf.* **2009**, *76*, 201.

(51) Humphrey, W.; Dalke, A.; Schulten, K. *J. Mol. Graphics* **1996**, *14*, 33.

(52) Frisch, M. J.; et al. *Gaussian 09, Revision B.1*, Gaussian, Inc.: Wallingford, CT, 2009.

(53) Becke, A. D. *J. Chem. Phys.* **1986**, *84*, 4524.

(54) Perdew, J. P. *Phys. Rev. B* **1986**, *33*, 8822.

(55) Jensen, K. P.; Ryde, U. *Coord. Chem. Rev.* **2009**, *253*, 769.

(56) Dapprich, S.; Komáromi, I.; Byun, K. S.; Morokuma, K.; Frisch, M. J. *J. Mol. Struct. (Theochem)* **1999**, *462*, 1.

(57) Vreven, T.; Byun, K. S.; Komáromi, I.; Dapprich, S.; Montgomery, J. A.; Morokuma, K.; Frisch, M. J. *J. Chem. Theory Comput.* **2006**, *2*, 815.

(58) Brown, K. L. *Chem. Rev.* **2005**, *105*, 2075.

(59) Dong, S.; Padmakumar, R.; Banerjee, R.; Spiro, T. G. *J. Am. Chem. Soc.* **1999**, *121*, 7063.

(60) Toraya, T.; Ishida, A. *Biochemistry* **1988**, *27*, 7677.

(61) Bresciani-Pahor, N.; Forcolin, M.; Marzilli, L. G.; Randaccio, L.; Summers, M. F.; Toscano, P. J. *Coord. Chem. Rev.* **1985**, *63*, 1.

2376

dx.doi.org/10.1021/ja210417k | *J. Am. Chem. Soc.* 2012, 134, 2367−2377

(62) Halpern, J. *Science* **1985**, *227*, 869.

(63) Loferer, M. J.; Webb, B. M.; Grant, G. H.; Liedl, K. R. *J. Am. Chem. Soc.* **2002**, *125*, 1072.

(64) Perilla, J. R.; Beckstein, O.; Denning, E. J.; Woolf, T. B. *J. Comput. Chem.* **2011**, *32*, 196.

(65) Marszalek, P. E.; Lu, H.; Li, H.; Carrion-Vazquez, M.; Oberhauser, A. F.; Schulten, K.; Fernandez, J. M. *Nature* **1999**, *402*, 100.

(66) Bui, J. M.; McCammon, J. A. *Proc. Natl. Acad. Sci. U.S.A.* **2006**, *103*, 15451.

(67) Ferrara, P.; Apostolakis, J.; Caflisch, A. *J. Phys. Chem. B* **2000**, *104*, 4511.

(68) Huang, H.; Ozkirimli, E.; Post, C. B. *J. Chem. Theory Comput.* **2009**, *5*, 1304.

(69) Brown, K. L.; Cheng, S.; Marques, H. M. *Polyhedron* **1998**, *17*, 2213.

(70) Hay, B. P.; Finke, R. G. *J. Am. Chem. Soc.* **1986**, *108*, 4820.

(71) Dölker, N.; Morreale, A.; Maseras, F. *J. Biol. Inorg. Chem.* **2005**, *10*, 509.

(72) Khoroshun, D. V.; Warncke, K.; Ke, S.-C.; Musaev, D. G.; Morokuma, K. *J. Am. Chem. Soc.* **2002**, *125*, 570.

(73) Altona, C.; Sundaralingam, M. *J. Am. Chem. Soc.* **1972**, *94*, 8205.

(74) Maity, A. N.; Hsieh, C.-P.; Huang, M.-H.; Chen, Y.-H.; Tang, K.-H.; Behshad, E.; Frey, P. A.; Ke, S.-C. *J. Phys. Chem. B* **2009**, *113*, 12161.

(75) Toogood, H. S.; Leys, D.; Scrutton, N. S. *FEBS J.* **2007**, *274*, 5481.